ENGINEERING TRANSACTIONS • *Engng. Trans.* • **63**, 4, 421–437, 2015
Polish Academy of Sciences • Institute of Fundamental Technological Research (IPPT PAN)
National Engineering School of Metz (ENIM) • Poznan University of Technology

Determination of Shear Modulus of Elasticity for Thin-Walled Trapezoidal Corrugated Cores of Seven-Layer Sandwich Plates

Jerzy LEWIŃSKI[1)], Ewa MAGNUCKA-BLANDZI[2)], Wacław SZYC[1)]

[1)] *Poznań University of Technology*
Institute of Applied Mechanics
Jana Pawła II 24, 60-965 Poznań, Poland
e-mail: {jerzy.lewinski, waclaw.szyc}@put.poznan.pl

[2)] *Poznań University of Technology*
Institute of Mathematics
Piotrowo 3A, 60-965 Poznań, Poland
e-mail: ewa.magnucka-blandzi@put.poznan.pl

Two thin-walled trapezoidal corrugated cores of seven-layer sandwich plate constitute the subject of this study. Transverse shear moduli of these cores are analytically determined and FEM numerically studied with the use of SOLIDWORKS software. The results of both methods are compared using a plate model.

Key words: sandwich plates, corrugated cores, elastic shear modulus.

1. Introduction

Strength and stability problems of thin-walled multilayer structures have been studied from the mid of the 20th century until today. Libove and Hubka [7] presented the first detailed analytical study of elastic constants for corrugated cores of sandwich plates. Allen [1] presented a comprehensive study regarding analysis and design of sandwich structures. Carlsson *et al.* [3] described the model of transverse shear stiffness for sandwich plate with corrugated core. Findings of their study were verified by experiments. Elastic constants for sandwich structures with corrugated core were calculated by Cheng *et al.* [4] based on finite element method (FEM) numerical analysis. The shear stiffness model for corrugated core structures was presented by Isaksson *et al.* [5] and its applicability was evaluated through experiments and finite element analysis. Peng *et al.* [11] proposed a mesh-free Galerkin method based on the first-order

shear deformation theory for the elastic bending analysis of corrugated plates. The results of calculations were compared with the results of a three-dimensional numerical analysis using ANSYS system. KAZEMAHVAZI and ZENKERT in [6] presented an original way of modelling corrugated sandwich structures. Their analytical model was described in detail and the results were compared to finite element prediction. MAGNUCKI *et al.* [10] analysed strength and buckling of sandwich beams with a crosswise or lengthwise corrugated core. The results of analytical and FEM numerical calculations as well as experimental results were described and compared in their study. BARTOLOZZI *et al.* [2] presented a general analytical method of determining equivalent properties for corrugated cores of sandwich structures. Their paper contains analytical formulation and its validation using FEM simulations. MAGNUCKA-BLANDZI and MAGNUCKI [8] presented the theoretical study of transverse shear modulus determination for corrugated cores of sandwich beams. Four corrugated cores in the form of circular arcs, a sin wave, trapezoids and an odd function were analysed. Their study shows considerable sensitivity of the shear modulus to shape of the corrugation. MAGNUCKA-BLANDZI *et al.* [9] described the mathematical modelling of transverse shearing effect for sandwich beams with sinusoidal crosswise and lengthwise corrugated cores. A distinct influence of shearing effect on deflections and critical loads was observed.

Two thin-walled trapezoidal corrugated cores of seven-layer sandwich plate (the main core and the face core) constitute the subject of this theoretical study (Fig. 1).

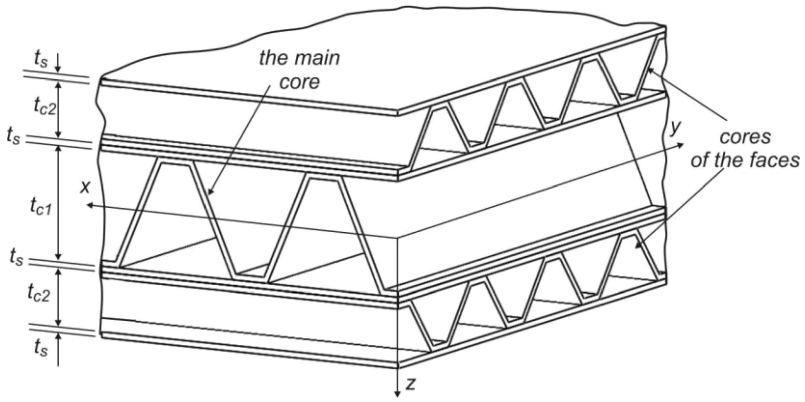

FIG. 1. Scheme of the seven-layer plate.

The trapezoidal corrugated main core connects two three-layer faces. The corrugation of the main core is orthogonal to the corrugations of the cores of faces. The total thickness of the plate is as follows:

$$t_p = t_{c1} + 2t_{c2} + 4t_s, \tag{1.1}$$

where t_{c1} is the depth of the main core, t_{c2} is the depth of the face core and t_s is the thickness of the sheets.

2. Analytical models of trapezoidal corrugated cores

2.1. The corrugated main core

The characteristic segment of the main corrugated core of the length b_{01} (the corrugation pitch of the main core) with two faces is shown in Fig. 2. The thickness of the corrugated sheet is t_{01}, the width of the flanges is b_{f1} and the width of the segment of the face core (i.e., the corrugation pitch of the face core) is b_{02}.

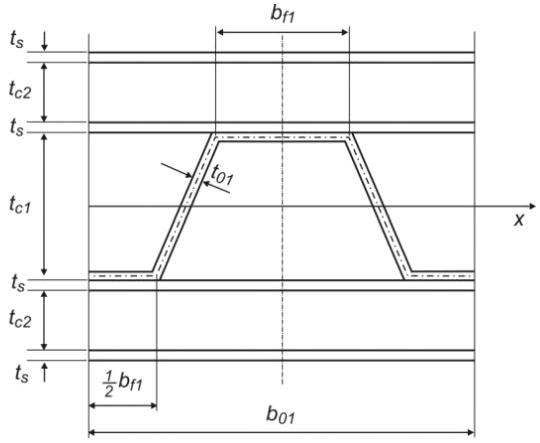

Fig. 2. Scheme of cross section of the main core for one corrugation pitch b_{01}.

The shear effect of the corrugated main core is a consequence of opposite x-displacements of the faces. It is assumed that the faces are rigid compared to the thin-walled corrugated sheet of the main core. The field of displacement is anti-symmetric (Fig. 3).

Thus, the analytical model includes a quarter of the pitch of the corrugated main core (Fig. 4).

The bending moment $M_b(s)$ and the normal force $N(s)$ in the plate with the trapezoidal main core of the width b_{02} are

$$M_b(s) = (F_s \sin\alpha_1 - R\cos\alpha_1)\, s, \qquad N(s) = F_s \cos\alpha_1 + R\sin\alpha_1, \tag{2.1}$$

where F_s is the load (shear force), R is the reactive force, s is the linear coordinate.

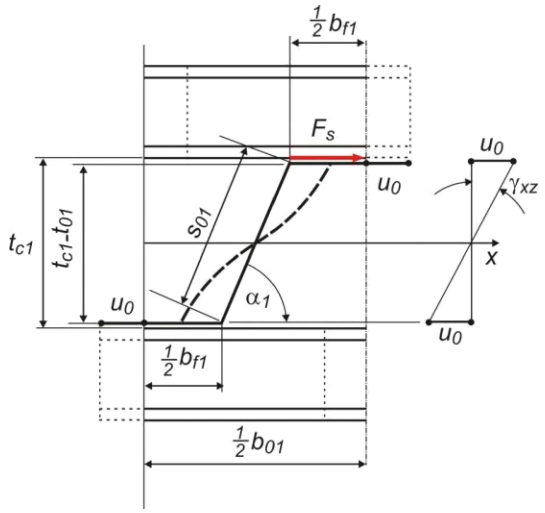

FIG. 3. Scheme of anti-symmetrical displacement for pure shear of the main core.

a) b)

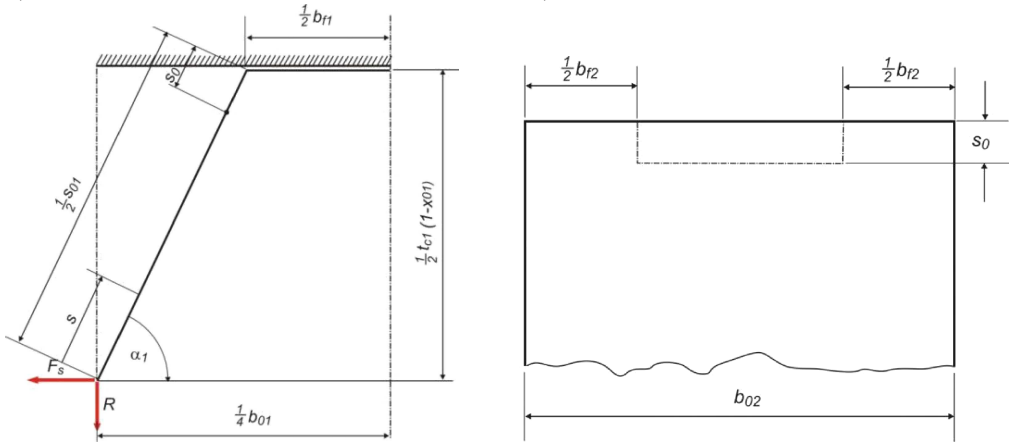

FIG. 4. Scheme of the theoretical model: a) load-forces, b) the auxiliary view.

Elastic strain energy is

$$U_\varepsilon = U_\varepsilon^{(b)} + U_\varepsilon^{(t)}, \tag{2.2}$$

where

$$U_\varepsilon^{(b)} = \frac{12\left(1-\nu^2\right)}{2Et_{01}^3}\left[\frac{1}{b_{02}}\int\limits_0^{\frac{1}{2}s_{a1}-s_0} M_b^2(s)ds + \frac{1}{b_{f2}}\int\limits_{\frac{1}{2}s_{a1}-s_0}^{\frac{1}{2}s_{a1}} M_b^2(s)ds\right] \text{ – bending energy,}$$

$$U_{\varepsilon}^{(t)} = \frac{1-\nu^2}{2Et_{01}}\left[\frac{1}{b_{02}}\int\limits_{0}^{\frac{1}{2}s_{a1}-s_0} N^2(s)ds + \frac{1}{b_{f2}}\int\limits_{\frac{1}{2}s_{a1}-s_0}^{\frac{1}{2}s_{a1}} N^2(s)ds\right] \text{ – tension energy,}$$

E – Young's modulus, ν – Poisson's ratio.

This energy is formulated according to Saint-Venant's principle with consideration of the elastic joint of the corrugated main core with rigid faces (Fig. 4b). The edge effect decays at the small length s_0. TIMOSHENKO and GOODIER [12] described and discussed this type of problem.

The following unknown reactive force is determined by considering the theorem of minimum potential energy (Menabrea's theorem) $\partial U_{\varepsilon}/\partial R = 0$:

$$R = \widetilde{R}F_s, \tag{2.3}$$

where the dimensionless reactive force is

$$\widetilde{R} = \frac{\alpha_{fs}}{\alpha_r}\sin\alpha_1\cos\alpha_1,$$

$$\alpha_{fs} = \left(\frac{1}{2}-x_{s0}\right)^3 + \frac{x_{s0}}{x_{f2}}\left(\frac{3}{4}-\frac{3}{2}x_{s0}+x_{s0}^2\right) - \left(\frac{x_{01}}{2\widetilde{s}_{a1}}\right)^2\left(\frac{1}{2}-x_{s0}+\frac{x_{s0}}{x_{f2}}\right), \tag{2.4}$$

$$\alpha_r = \left[\left(\frac{1}{2}-x_{s0}\right)^3 + \frac{x_{s0}}{x_{f2}}\left(\frac{3}{4}-\frac{3}{2}x_{s0}+x_{s0}^2\right)\right]\cos^2\alpha_1 + \left(\frac{x_{01}}{2\widetilde{s}_{a1}}\right)^2\left(\frac{1}{2}-x_{s0}+\frac{x_{s0}}{x_{f2}}\right)\sin^2\alpha_1,$$

and other parameters are

$$x_{01} = \frac{t_{01}}{t_{c1}}, \qquad x_{b1} = \frac{b_{01}}{t_{c1}},$$

$$x_{f1} = \frac{b_{f1}}{b_{01}}, \qquad s_{a1} = t_{c1}\widetilde{s}_{a1},$$

$$\widetilde{s}_{a1} = \sqrt{(1-x_{01})^2 + x_{b1}^2\left(\frac{1}{2}-x_{f1}\right)^2}, \qquad x_{s0} = \frac{s_0}{s_{a1}},$$

$$s_0 = k_{s0}b_{f2}, \qquad x_{f2} = \frac{b_{f2}}{b_{02}},$$

$$k_{s0}(x_{f1}) = \frac{1}{5}(2+23\,x_{f1}).$$

The unknown displacement u_0 (Fig. 3) based on the Castigliano theorem with consideration of the expressions (2.1) and (2.2) is as follows:

$$u_0 = \frac{\partial U_\varepsilon}{\partial F_s} = 4\frac{1-\nu^2}{Eb_{02}}\left(\frac{\widetilde{s}_{a1}}{x_{01}}\right)^3 f_u F_s, \tag{2.5}$$

where $f_u = f_{u1} + f_{u2}$, and

$$f_{u1} = \left[\left(\frac{1}{2} - x_{s0}\right)^3 + \frac{x_{s0}}{x_{f2}}\left(\frac{3}{4} - \frac{3}{2}x_{s0} + x_{s0}^2\right)\right]\left(\sin^2\alpha_1 - \widetilde{R}\sin\alpha_1\cos\alpha_1\right),$$

$$f_{u2} = \left(\frac{x_{01}}{2\widetilde{s}_{a1}}\right)^2\left(\frac{1}{2} - x_{s0} + \frac{x_{s0}}{x_{f2}}\right)\left(\cos^2\alpha_1 + \widetilde{R}\sin\alpha_1\cos\alpha_1\right).$$

The shear strain angle γ_{xz} and the shear stress τ_{xz} (Fig. 3) are as follows:

$$\gamma_{xz} = \frac{2u_0}{t_{c1}(1-x_{01})}, \qquad \tau_{xz} = \frac{2F_s}{b_{01}b_{02}}. \tag{2.6}$$

Thus, the shear modulus of elasticity (the Hooke's law) for the corrugated main core is in the following form:

$$G_{xz}^{(C1)} = \frac{\tau_{xz}}{\gamma_{xz}} = \widetilde{G}_{xz}^{(C1)}E, \tag{2.7}$$

where the dimensionless shear modulus is

$$\widetilde{G}_{xz}^{(C1)} = \frac{\tau_{xz}}{\gamma_{xz}} = \frac{1-x_{01}}{4\,(1-\nu^2)\,x_{b1}f_u}\left(\frac{x_{01}}{\widetilde{s}_{a1}}\right)^3. \tag{2.8}$$

EXAMPLE. The parameters of the structure are: $t_s = 0.8$ mm, $t_{c1} = 31.4$ mm, $t_{01} = 0.8$ mm, $b_{01} = 46.0$ mm, $b_{f1} = 10.0$ mm, $t_{c2} = 16.2$ mm, $t_{02} = 0.8$ mm, $b_{02} = 40.0$ mm and $b_{f2} = 8.0$ mm.

The value of the dimensionless shear modulus for the above data is $\widetilde{G}_{xz}^{(C1} = 0.001459$.

2.2. The corrugated core of the faces

The characteristic segment of the trapezoidal corrugated core of the faces for one pitch b_{02} is shown in Fig. 5. The thickness of the corrugated sheet is t_{02}, the width of flanges is b_{f2} and the segment is of unit width.

The shear effect of the corrugated face core is a consequence of a y-displacement of the sheet. It is assumed that the main core is rigid compared to the thin-walled corrugated sheet of the face core. The field of displacement is shown in Fig. 6.

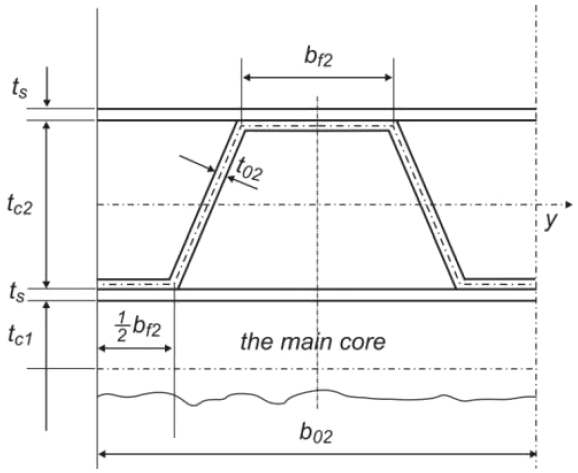

FIG. 5. Scheme of cross section of the face corrugated core for one corrugated pitch b_{02}.

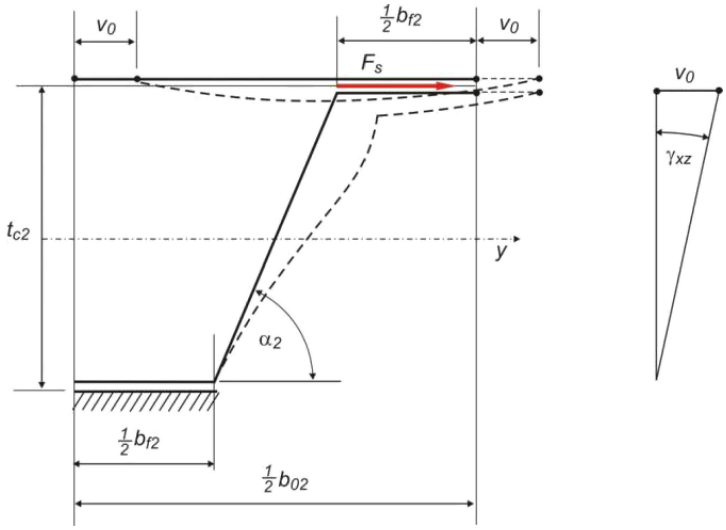

FIG. 6. Scheme of displacement for pure shear of the face core.

Thus, the force system acting in the corrugated face core and in the outer sheet is shown in Fig. 7.

The bending moments and normal forces for the system are as follows:

- the first range $\left\{0 \leq s_1 \leq \frac{1}{2}b_{02}\,(1 - x_{f2})\right\}$

$$M_b(s_1) = R_1 s_1, \tag{2.9}$$

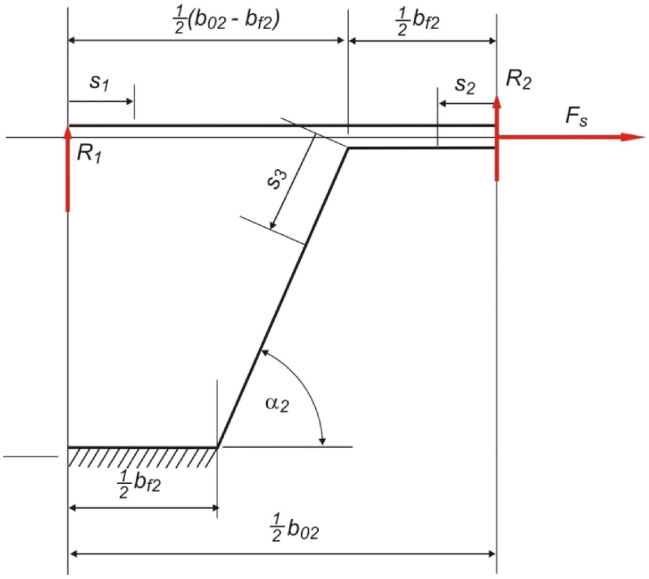

FIG. 7. Scheme of the force system.

- the second range $\left\{0 \leq s_2 \leq \frac{1}{2} b_{02} x_{f2}\right\}$

$$M_b(s_2) = R_2 s_2, \tag{2.10}$$

- the third range $\{0 \leq s_3 \leq s_{a2}\}$

$$M_b(s_3) = -R_1 \left[\frac{1}{2} b_{02} (1 - x_{f2}) - s_3 \cos\alpha_2\right] + R_2 \left[\frac{1}{2} b_{02} x_{f2} + s_3 \cos\alpha_2\right] - F_s s_3 \sin\alpha_2, \tag{2.11}$$

$$N(s_3) = (R_1 + R_2) \sin\alpha_2 + F_s \cos\alpha_2, \tag{2.12}$$

where

$$s_{a2} = t_{c2} \widetilde{s}_{a2}, \qquad \widetilde{s}_{a2} = \sqrt{(1 - x_{02})^2 + x_{b2}^2 \left(\frac{1}{2} - x_{f2}\right)^2}.$$

Equation of elastic strain energy is as follows:

$$U_\varepsilon = U_\varepsilon^{(1)} + U_\varepsilon^{(2)} + U_\varepsilon^{(3)}, \tag{2.13}$$

where

$$U_{\varepsilon}^{(1)} = \frac{12(1-\nu^2)}{2Et_s^3} \int_0^{\frac{1}{2}b_{02}(1-x_{f2})} M_b^2(s_1)ds_1,$$

$$U_{\varepsilon}^{(2)} = \frac{12(1-\nu^2)}{2E(t_s+t_{02})^3} \int_0^{\frac{1}{2}b_{02}x_{f2}} M_b^2(s_2)ds_2,$$

$$U_{\varepsilon}^{(3)} = \frac{12(1-\nu^2)}{2Et_{02}^3} \int_0^{s_{a2}} M_b^2(s_3)ds_3 + \frac{1-\nu^2}{2Et_{02}} \int_0^{s_{a2}} N^2(s_3)\,ds_3.$$

The following two algebraic equations are obtained based on the theorem of minimum potential energy (Menabrea's theorem) $\partial U_{\varepsilon}/\partial R_1 = 0$ and $\partial U_{\varepsilon}/\partial R_2 = 0$:

$$-a_{11}R_1 + a_{12}R_2 = \beta_1 F_s, \qquad -a_{21}R_1 + a_{22}R_2 = \beta_2 F_s, \tag{2.14}$$

from which $R_1 = \widetilde{R}_1 F_s$, $R_2 = \widetilde{R}_2 F_s$, where

$$\widetilde{R}_1 = \frac{a_{12}\beta_2 - a_{22}\beta_1}{a_{11}a_{22} - a_{12}^2}, \qquad \widetilde{R}_2 = \frac{a_{11}\beta_2 - a_{12}\beta_1}{a_{11}a_{22} - a_{12}^2}, \tag{2.15}$$

and

$$a_{111} = \frac{x_{02}}{2\widetilde{s}_{a2}}\left[(1-x_{f2})\,x_{b2}\frac{x_2}{x_1}\right]^3 + \left(\frac{x_{b2}}{x_{02}}\right)^2\left[3\,(1-x_{f2})^2 - 6\,(1-x_{f2})\,\frac{\widetilde{s}_{a2}}{x_{b2}}\cos\alpha_2 + 4\left(\frac{\widetilde{s}_{a2}}{x_{b2}}\cos\alpha_2\right)^2\right],$$

$$a_{11} = a_{111} + \sin^2\alpha_2, \qquad a_{21} = a_{12}, \qquad x_1 = \frac{t_s}{t_{c1}},$$

$$x_2 = \frac{t_{c2}}{t_{c1}}, \qquad x_{b2} = \frac{b_{02}}{t_{c2}},$$

$$x_{02} = \frac{t_{02}}{t_{c2}}, \qquad x_{f2} = \frac{b_{f2}}{b_{02}},$$

$$a_{12} = \left(\frac{x_{b2}}{x_{02}}\right)^2\left[3x_{f2}\,(1-x_{f2}) + 3\,(1-2x_{f2})\,\frac{\widetilde{s}_{a2}}{x_{b2}}\cos\alpha_2 - 4\left(\frac{\widetilde{s}_{a2}}{x_{b2}}\cos\alpha_2\right)^2\right] - \sin^2\alpha_2,$$

$$a_{22} = \frac{x_{02}}{2\widetilde{s}_{a2}} \left(\frac{x_2 x_{f2} x_{b2}}{x_1 + x_2 x_{02}} \right)^3 + \left(\frac{x_{b2}}{x_{02}} \right)^2 \left[3x_{f2}^2 + 6x_{f2} \frac{\widetilde{s}_{a2}}{x_{b2}} \cos\alpha_2 + 4 \left(\frac{\widetilde{s}_{a2}}{x_{b2}} \cos\alpha_2 \right)^2 \right] + \sin^2\alpha_2,$$

$$\beta_1 = \left\{ \left(\frac{x_{b2}}{x_{02}} \right)^2 \frac{\widetilde{s}_{a2}}{x_{b2}} \left[3\left(1 - x_{f2}\right) - 4 \frac{\widetilde{s}_{a2}}{x_{b2}} \cos\alpha_2 \right] + \cos\alpha_2 \right\} \sin\alpha_2,$$

$$\beta_2 = \left\{ \left(\frac{x_{b2}}{x_{02}} \right)^2 \frac{\widetilde{s}_{a2}}{x_{b2}} \left[3x_{f2} + 4 \frac{\widetilde{s}_{a2}}{x_{b2}} \cos\alpha_2 \right] - \cos\alpha_2 \right\} \sin\alpha_2.$$

The unknown displacement v_0 (Fig. 3) based on the Castigliano theorem with consideration of the expression (2.13) is as follows:

$$v_0 = \frac{\partial U_\varepsilon}{\partial F_s} = \frac{1 - \nu^2}{E} \left(\frac{\widetilde{s}_{a2}}{x_{02}} \right)^3 f_v F_s, \tag{2.16}$$

where $f_v = f_{v1} + f_{v2}$, and

$$f_{v1} = \left\{ \widetilde{R}_1 \left[3\left(1 - x_{f2}\right) \frac{x_{b2}}{\widetilde{s}_{a2}} - 4\cos\alpha_2 \right] - \widetilde{R}_2 \left[3x_{f2} \frac{x_{b2}}{\widetilde{s}_{a2}} + 4\cos\alpha_2 \right] + 4\sin\alpha_2 \right\} \sin\alpha_2,$$

$$f_{v2} = \left(\frac{x_{02}}{\widetilde{s}_{a2}} \right)^2 \left[\left(\widetilde{R}_1 + \widetilde{R}_2 \right) \sin\alpha_2 + \cos\alpha_2 \right] \cos\alpha_2.$$

The shear strain angle γ_{yz} and the shear stress τ_{yz} (Fig. 6) are as follows:

$$\gamma_{yz} = \frac{v_0}{t_{c2}}, \qquad \tau_{yz} = \frac{2F_s}{b_{02}}. \tag{2.17}$$

Thus, the shear modulus of elasticity (the Hooke's law) for the corrugated face core is in the following form:

$$G_{yz}^{(C2)} = \frac{\tau_{yz}}{\gamma_{yz}} = \widetilde{G}_{yz}^{(C2)} E, \tag{2.18}$$

where the dimensionless shear modulus is

$$\widetilde{G}_{yz}^{(C2)} = \frac{\tau_{yz}}{\gamma_{yz}} = \frac{2}{\left(1 - \nu^2\right) x_{b2} f_v} \left(\frac{x_{02}}{\widetilde{s}_{a2}} \right)^3. \tag{2.19}$$

EXAMPLE. Parameters of the structure: $t_s = 0.8$ mm, $t_{c1} = 31.4$ mm, $t_{01} = 0.8$ mm, $b_{01} = 46.0$ mm, $b_{f1} = 10.0$ mm, $t_{c2} = 16.2$ mm, $t_{02} = 0.8$ mm, $b_{02} = 40.0$ mm and $b_{f2} = 8.0$ mm.

The value of the dimensionless shear modulus for the above data is $\widetilde{G}_{yz}^{(C2)} = 0.0009895$.

3. FEM Numerical models of trapezoidal corrugated cores

In order to estimate accuracy of the above analytical analysis the considered plate is modelled with the SOLIDWORKS software using the example data. The SOLIDWORKS model is confined to a single segment of the plate, including a single, periodically repeated trapezoidal shape in each of the cores, i.e., in the main and facial cores.

3.1. The corrugated main core

The apparent transverse shear modulus of the plate is determined with the help of the model shown in Fig. 8. Behaviour of the plate subject to shearing in x-direction is depicted by loading the bottom surface of the upper face with a tangent force in x-direction and the upper surface of the bottom face with a force of equal value in the opposite direction. The ratio of x-displacement of the surfaces to the distance between them is equal to the plate transverse strain. Therefore, due to asymmetry of the model only a half of the total plate thickness is taken into account.

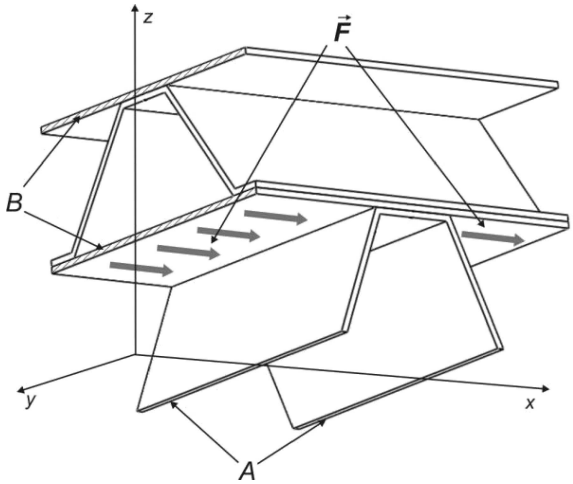

Fig. 8. The SOLIDWORKS model adopted for the purpose of determination of the apparent transverse shear modulus $G_{xz}^{(C1-FEM)}$.

Hence, the model consists of the upper face which is composed of two walls separated by the face core located between them and a half of the main core located above the xy-plane. The bottom surface of the upper face is loaded with a tangent force 1 kN in x-direction. The x, y, and z displacements of the trapezoid A edges located at the xy-plane are equal to zero, while the B edges are fixed only in y and z directions (Fig. 8).

The model subjected to the above mentioned load and boundary conditions is displaced as shown in Fig. 9.

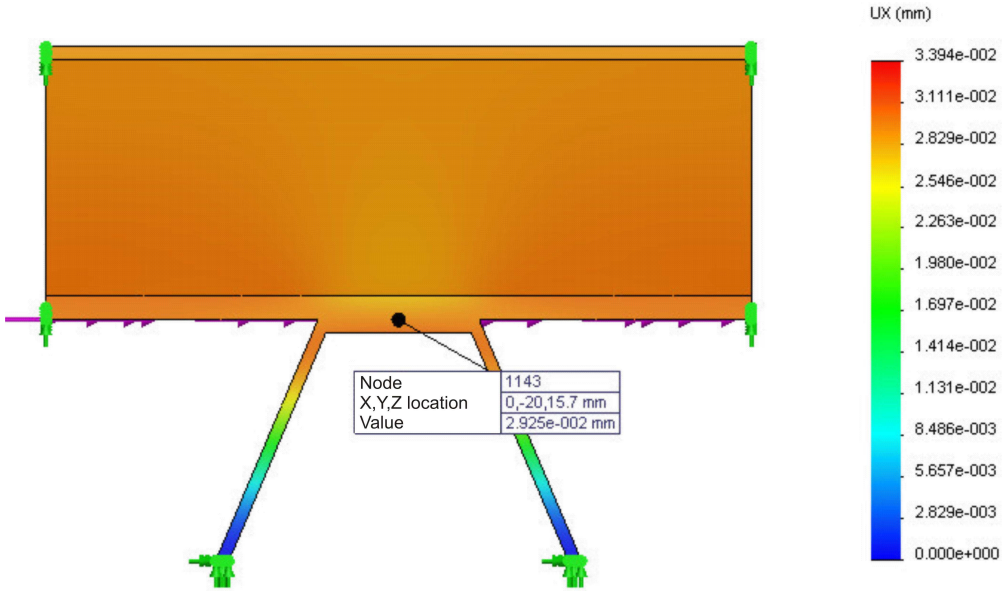

FIG. 9. Tangent displacement of the main core of the considered seven-layer plate – the bottom surface of the upper face subjected to a tangent force equal to 1 kN acting in x-direction (a half of the total plate thickness is considered).

Middle point of the bottom face surface is displaced by $\delta_{x0} = 3.005 \cdot 10^{-2}$ mm. Hence, the plate transverse strain is equal to

$$\gamma_{xz} = 2\frac{\delta_{x0}}{t_{c1}} = 2\frac{2.925 \cdot 10^{-2}}{31.4} = 1.863 \cdot 10^{-3}. \tag{3.1}$$

Since the force is applied to the rectangular surface $A_S = b_{01} \cdot b_{02} = 46$ mm $\cdot$ 40 mm $= 1840$ mm^2, the transverse shear modulus of the plate in x-direction is equal to

$$G_{xz}^{(C1-FEM)} = \frac{\tau_{xz}}{\gamma_{xz}} = \frac{F}{A_s \cdot \gamma_{xz}} = \frac{1000}{1840 \cdot 1.863 \cdot 10^{-3}} \frac{N}{\text{mm}^2} = 291.713 \text{ MPa}. \tag{3.2}$$

Hence, the relative shear modulus is

$$\widetilde{G}_{xz}^{(C1-FEM)} = G_{xz}^{(C1-FEM)} \Big/ E = 0.001459. \tag{3.3}$$

3.2. The corrugated core of the faces

A similar approach enables to determine the plate transverse shear modulus in y-direction.

Using a similar model allows to calculate the apparent transverse shear modulus of the plate in y-direction (Fig. 10). In this case, the bottom surface of upper layer of the upper face is loaded with a tangent force 1 kN in y-direction. The x, y, and z displacements of the A-edges are equal to zero, while the B-edges are fixed in x and z directions (Fig. 10).

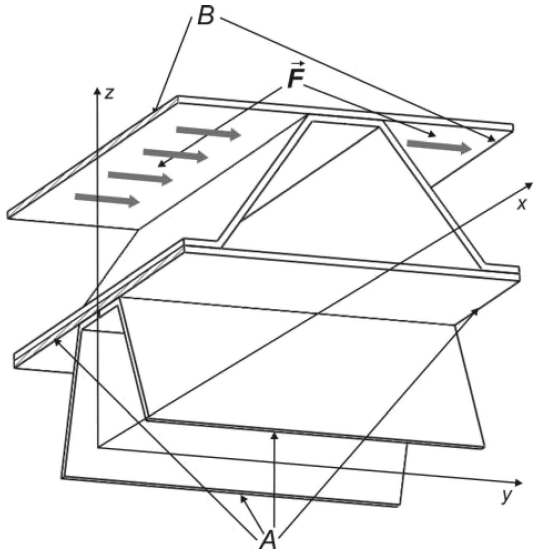

FIG. 10. The SOLIDWORKS model adopted for the purpose of determination of the apparent transverse shear modulus in y-direction.

The model bearing such load and boundary conditions is displaced as shown in Fig. 11.

Middle point of the bottom surface of the upper layer is displaced by $\delta_{y0} = 4.127 \cdot 10^{-2}$ mm. Hence, the plate transverse strain is equal to

$$\gamma_{yz} = \frac{\delta_{y0}}{t_{c2}} = \frac{4.834 \cdot 10^{-2} - 5.430 \cdot 10^{-3}}{16.2} = 2.6488 \cdot 10^{-3}. \tag{3.4}$$

The force is applied as before to the same rectangular surface of the area equal to 1840 mm^2. The transverse shear modulus of the plate in x-direction is

$$G_{yz}^{(C2-FEM)} = \frac{\tau_{yz}}{\gamma_{yz}} = \frac{F}{A_s \cdot \gamma_{yz}} = \frac{1000}{1840 \cdot 2.6488 \cdot 10^{-3}} \frac{N}{\text{mm}^2} = 205.182 \text{ MPa}, \tag{3.5}$$

Hence, the relative shear modulus is

$$\widetilde{G}_{yz}^{(C2-FEM)} = G_{yz}^{(C2-FEM)} \Big/ E = 0.001026. \tag{3.6}$$

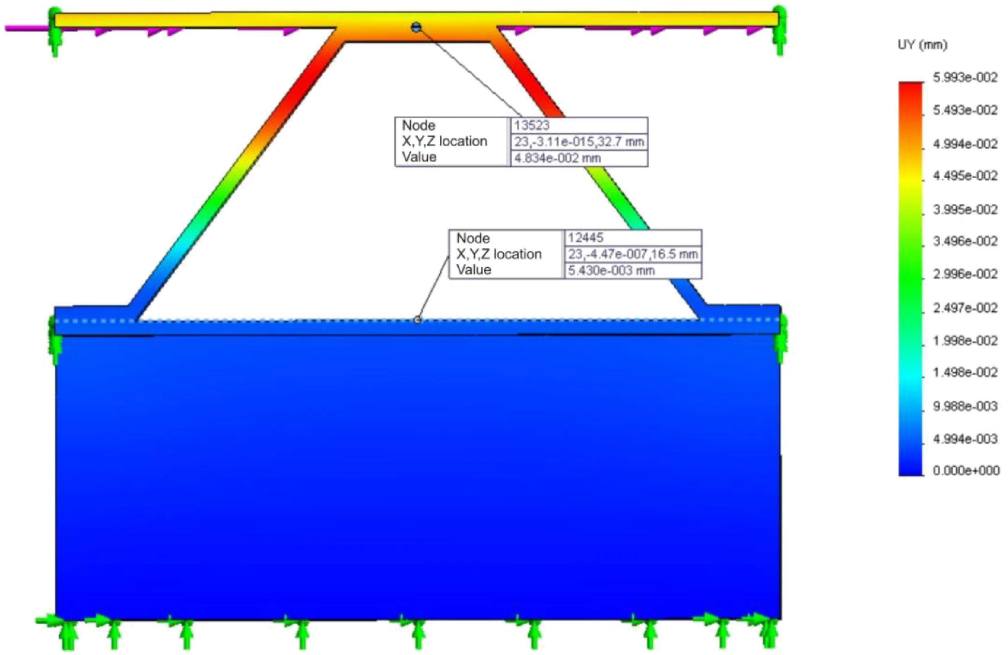

FIG. 11. Tangent displacement of the main core of the considered seven-layer plate – the bottom surface of the upper face subjected to tangent force equal to 1 kN acting in y-direction.

Comparison of the results obtained analytically and numerically shows good compliance:

$$\begin{aligned} &\widetilde{G}_{xz}^{(C1-Analyt)} = 0.001387, \qquad \widetilde{G}_{xz}^{(C1-FEM)} = 0.001420, \\ &\widetilde{G}_{yz}^{(C2-Analyt)} = 0.0009895, \qquad \widetilde{G}_{yz}^{(C2-FEM)} = 0.001026, \end{aligned} \tag{3.7}$$

since the differences between them are below 4 percent.

However, in order to improve credibility of the results some additional variants of the sandwich plates were considered. They differed in the area of the surfaces, where the cores are adjacent to planar faces. Two series of variants were studied: in the first one the shapes of the main cores varied ($b_{f1} = 8$, 9, 10, 11, 12 mm) while the cores of the faces remained unchanged ($b_{f2} = 8$ mm). The results of these examples are presented in Table 1 and Fig. 12a.

In the second series the cores of the faces were changed ($b_{f2} = 6$, 7, 8, 9, 10 mm) with constant $b_{f1} = 10$ mm and the results are shown in Table 2 and Fig. 12b.

Such shape changes would affect the cross section areas of the cores; therefore, in order to keep them constant the thicknesses t_{01} and t_{02} were adjusted accordingly.

Table 1. Comparison of analytical and FEM numerical results obtained for various variants of the main core (determined by b_{f1} and t_{01} parameters).

b_{f1} [mm]	8	9	10	11	12
t_{01} [mm]*	0.82261	0.81138	0.8	0.78847	0.77679
$\widetilde{G}_{xz}^{C1}$ [Analytic.]	0.002106	0.001761	0.001459	0.001195	0.000966
$\widetilde{G}_{xz}^{C1}$ [FEM]	0.002160	0.001772	0.001459	0.001198	0.0009826

* The thickness t_{01} is adjusted to keep cross section area of the main core constant.

Table 2. Comparison of analytical and FEM numerical results obtained for various variants of the face corrugated core (determined by b_{f2} and t_{02} parameters).

b_{f2}[mm]	6	7	8	9	10
t_{02} [mm]*	0.82169	0.81114	0.8	0.78821	0.77578
$\widetilde{G}_{yz}^{C2}$ [Analytic.]	0.001858	0.001338	0.0009895	0.0007466	0.0005717
$\widetilde{G}_{yz}^{C2}$ [FEM]	0.001976	0.001392	0.001026	0.0007471	0.0005570

* The thickness t_{02} is adjusted to keep cross section area of the face corrugated core constant.

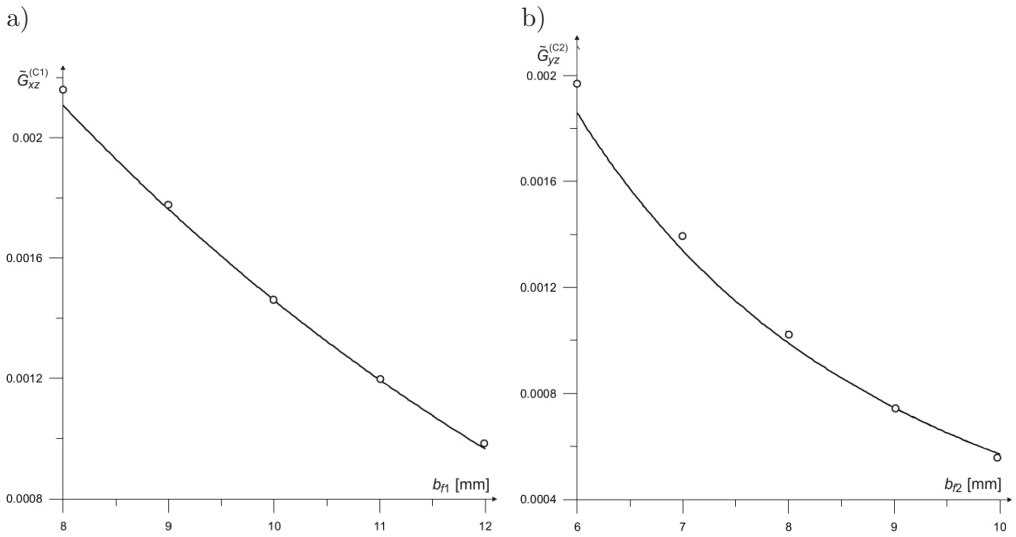

FIG. 12. Comparison of analytical (solid line) and FEM numerical (circles) results obtained for a) various variants of the main core and b) various variants of the face corrugated core.

Compliance of analytical and numerical results remains good. In the first series of the variants it is below 3 percent. The second series gave worse compliance amounting to 13.7% in the worst case for $b_{f2} = 6$ mm.

4. Conclusion

The considered seven-layer plate is a complex thin-walled structure and, therefore, a full analytical description of the shear effect of the cores is very complicated. In the present paper, the analytical model includes a certain simplification: the elastic joints between the main core corrugated sheet and the faces are simplified using the Saint-Venant's principle.

The analytical and FEM numerical studies presented in this paper give evidence that the width of the core trapezoidal base significantly affects the equivalent shear modulus of the core. The detailed results of the study are presented in Tables 1 and 2 and in Fig. 12.

Hence, the shear moduli defined by Eq. (2.8) for the main core and by Eq. (2.19) for the face core can be used for modelling of seven-layer rectangular plates.

Acknowledgment

The project was funded by the National Science Centre allocated on the basis of the decision number DEC-2013/09/B/ST8/00170.

References

1. Allen H.G., *Analysis and design of structural sandwich panels*, Pergamon Press, UK, USA, Canada, Australia, France, Germany, 1969.
2. Bartolozzi G., Baldanzini N., Pierini M., *Equivalent properties for corrugated cores of sandwich structures. A general analytical method*, Composite Structures, **108**, 736–746, 2014.
3. Carlsson LA., Nordstrand T., Westerlind B., *On the elastic stiffnesses of corrugated core sandwich*, Journal of Sandwich Structures and Materials, **3**, 4, 253–267, 2001.
4. Cheng Q.H., Lee H.P., Lu C., *A numerical analysis approach for evaluating elastic constants of sandwich structures with various cores*, Composite Structures, **74**, 2, 226–236, 2006.
5. Isaksson P., Krusper A., Gradin P.A., *Shear correction factor for corrugated core structures*, Composite Structures, **80**, 1, 123–130, 2007.
6. Kazemahvazi S., Zenkert D., *Corrugated all-composite sandwich structures, Part 1: Modeling*, Composites Science and Technology, **69**, 7–8, 913–919, 2009.
7. Libove C., Hubka R.E., *Elastic constants for corrugated-core. Sandwich plates*, Technical Note 2289, NACA, Washington, D.C., 1951.
8. Magnucka-Blandzi E., Magnucki K., *Transverse shear modulus of elasticity for thin-walled corrugated cores of sandwich beams. Theoretical study*, Journal of Theoretical and Applied Mechanics, **52**, 4, 971–980, 2014.

9. Magnucka-Blandzi E., Magnucki K., Wittenbek L., *Mathematical modelling of shearing effect for sandwich beams with sinusoidal corrugated cores*, Applied Mathematical Modelling, **39**, 9, 2796–2808, 2015.

10. Magnucki K., Jasion P., Kruś M., Kuligowski P., Wittenbeck L., *Strength and buckling of sandwich beams with corrugated core*, Journal of Theoretical and Applied Mechanics, **51**, 1, 15–24, 2013.

11. Peng L.X., Liew K.M., Kitipornchai S., *Analysis of stiffened corrugated plates based on the FSDT via the mesh-free method*, International Journal of Mechanical Sciences, **49**, 3, 364–378, 2007.

12. Timoshenko S., Goodier J.N., *Theory of Elasticity*, McGraw-Hill Book Company, New York, Toronto, London, 1951.

Received 8 April, 2015; accepted version June 27, 2015.